

# Lawrence Berkeley National Laboratory

## Recent Work

### Title

SUPERCONDUCTING PROPERTIES OF LIQUID PHASE SINTERED Nb-Nb<sub>3</sub>Sn AND HOT PRESSED Nb<sub>3</sub>Sn-NbC COMPACTS

### Permalink

<https://escholarship.org/uc/item/89c4j3pz>

### Authors

Goolsby, R.D.

Jones, R.H.

Zackay, T.F.

et al.

### Publication Date

1970

c.2

RECEIVED  
LAWRENCE  
RADIATION LABORATORY

APR 24 1970

LIBRARY AND  
DOCUMENTS SECTION

SUPERCONDUCTING PROPERTIES OF LIQUID PHASE SINTERED  
Nb-Nb<sub>3</sub>Sn AND HOT PRESSED Nb<sub>3</sub>Sn-NbC COMPACTS

R. D. Goolsby, R. H. Jones, V. F. Zackay, and E. R. Parker

January 1970

AEC Contract No. W-7405-eng-48

TWO-WEEK LOAN COPY

*This is a Library Circulating Copy  
which may be borrowed for two weeks.  
For a personal retention copy, call  
Tech. Info. Division, Ext. 5545*

LAWRENCE RADIATION LABORATORY  
UNIVERSITY of CALIFORNIA BERKELEY

UCRL-19178

25

## **DISCLAIMER**

This document was prepared as an account of work sponsored by the United States Government. While this document is believed to contain correct information, neither the United States Government nor any agency thereof, nor the Regents of the University of California, nor any of their employees, makes any warranty, express or implied, or assumes any legal responsibility for the accuracy, completeness, or usefulness of any information, apparatus, product, or process disclosed, or represents that its use would not infringe privately owned rights. Reference herein to any specific commercial product, process, or service by its trade name, trademark, manufacturer, or otherwise, does not necessarily constitute or imply its endorsement, recommendation, or favoring by the United States Government or any agency thereof, or the Regents of the University of California. The views and opinions of authors expressed herein do not necessarily state or reflect those of the United States Government or any agency thereof or the Regents of the University of California.

SUPERCONDUCTING PROPERTIES OF LIQUID PHASE SINTERED  
Nb-Nb<sub>3</sub>Sn AND HOT PRESSED Nb<sub>3</sub>Sn-NbC COMPACTS

R. D. Goolsby, R. H. Jones, V. F. Zackay, and E. R. Parker

Inorganic Materials Research Division, Lawrence Radiation Laboratory  
Department of Materials Science and Engineering, College of Engineering,  
University of California, Berkeley, California

ABSTRACT

The properties of several bulk superconductors prepared by two powder metallurgical techniques are shown to be related to the morphology, distribution and composition of the superconducting phase (Nb<sub>3</sub>Sn). In one technique, liquid tin was infiltrated into a porous niobium compact (liquid phase sintering), and in the second, a mixture of tin, niobium and carbon powders was hot pressed. The critical temperatures,  $T_c$ , upper critical fields,  $H_{c2}$ , and critical current densities,  $J_{cN}$ , were measured. The superconducting property found most sensitive to microstructural variations was that of current carrying capacity. The microstructures of specimens having the highest values of  $J_{cN}$  were characterized by a uniformly distributed network of Nb<sub>3</sub>Sn surrounding other phases.

## INTRODUCTION

Research in high field superconductivity for the past decade has been concentrated in two areas, a search for new materials (in either the bulk or thin film configurations), and the improvement of commercial superconductors. A steady improvement in the properties of commercial products has been achieved with composite structures, and also by the control of composition, microstructure and defect structure of the superconducting material itself. The research reported herein was a further attempt to enhance the superconducting properties of  $Nb_3Sn$  by optimizing the microstructure.

The specific objective of this study was to prepare bulk superconductors with  $Nb_3Sn$  present in the form of a network surrounding a second phase. The number of current carrying paths per unit of cross-sectional area was changed by altering processing variables. The techniques used varied the current carrying capacity while maintaining a high critical temperature,  $T_c$ , and a high upper critical field,  $H_{c2}$ . Materials were prepared by two methods. In one liquid tin was infiltrated into a pre-sintered, porous niobium compact, and in the other mixed powders of tin, niobium, and carbon were hot pressed. The critical temperature, critical current density, and upper critical field of the specimens were measured. The compositions and structures of these specimens were examined by X-ray diffraction, optical metallography and electron probe microanalysis.

### Specimen Preparation

The hot pressed specimens were prepared by pressing niobium, carbon, and tin powders mixed in the ratio of 6:4:3 respectively. The purity levels and powder sizes of the raw materials are shown in Table I. The powder mixture was blended in a rotating jar, placed in a double-acting graphite die, and simultaneously pressed and heated in a vacuum. The dimensions of the sintered specimens were 3 x 3 x 10 mm. The die temperatures were measured, with an estimated accuracy of  $\pm 50^{\circ}\text{C}$ , with an optical pyrometer. Schematics illustrating two variations of the sintering treatments used are shown in Fig. 1.

The other type of specimen was prepared by infiltrating a porous niobium compact with liquid tin (liquid phase sintering) in a vacuum. The porous niobium compact was produced by hot pressing coarse niobium powder (+200 mesh) at  $1400^{\circ}\text{C}$  for 30 minutes with a pressure of 1000 psi. Tin powder was then placed in the space above the compact in the graphite die, and the compact was infiltrated with tin by heating the die at  $800^{\circ}\text{C}$  ( $T_1$ ) at a pressure of 1000 psi for 15 minutes. Finally, the die temperature was increased to approximately  $1050^{\circ}\text{C}$  ( $T_2$ ) for 2 to 3 minutes with the pressure still applied, as shown schematically in Fig. 2. The resulting specimens had approximately the same dimensions as those of hot pressed specimens.

Shown in Table II is a summary of the processing treatments used in this research. The hot pressed specimens are numbered 1 through 9, and the infiltrated ones 10 and 11.

### Phase Identification

The microstructural phases were identified by X-ray diffraction analysis, optical metallography, and electron probe microanalysis. Metallographic identification was aided by anodization, using Picklesimer's solution.<sup>1</sup>

By maintaining standard anodizing conditions (27 volts, 6 minutes), constant phase-color relationships were obtained. The microanalysis was done on non-anodized specimens. These results are shown in Table III.

#### Critical Temperature Measurements

The superconducting transition temperature,  $T_c$ , was measured by a method described by Nembach.<sup>2</sup> This method consists of observing the change in mutual inductance of two coaxial coils surrounding a specimen as it passes through the critical temperature. The coaxial coils were wound as primary and secondary, with the voltage of the secondary being amplified and plotted on a multichannel recorder. A germanium resistance thermometer located near the specimen was used to measure the temperature. The germanium resistor was calibrated between 14 and 20°K against the vapor pressure of normal hydrogen.

The critical temperature,  $T_c$ , was defined as the temperature at which the secondary coil voltage was the average of the voltages for the completely normal and completely superconducting states of the specimen. The width of the transition,  $\Delta T_c$ , was defined as the temperature difference corresponding to 10 and 90% of the total secondary coil voltage change. The critical temperatures are shown in Table IV. The accuracy of these measurements is estimated to be  $\pm 0.1^\circ\text{K}$ .

#### Critical Current and Field Measurement

The critical currents and upper critical fields of the specimens were measured at 4.2°K using a pulsed magnetic field technique.<sup>3</sup> The spark-cut specimens had dimensions that were typically 2.1 x 1.0 x 10. mm. The specimen was mounted on the test probe such that the applied magnetic field was perpendicular to the direction

of the current through the specimen. The current pulse was started prior to the magnetic one and then stopped at the peak field to reduce heating. (The magnet rise time was 10 msec and the maximum field available was 220 kG.) The change in the voltage drop across the specimen and the magnetic field change were followed with a dual beam oscilloscope. A schematic of a typical Polaroid film record is shown in Fig. 3. The voltage induced by the pulsed magnetic field in the specimen and the attached wires, at zero specimen current, was also recorded on the Polaroid film. The latter curve was subtracted from the aforementioned curve to obtain a corrected curve for the condition when the current was passed through the specimen. The critical current densities and upper critical fields are given in Table IV.



## DISCUSSION

The properties of the bulk superconductors were interpreted in terms of microstructure and composition. The processing technique employed established the microstructure. The influence of several process variables on the microstructure are summarized below. The objective in all cases was to obtain a microstructure wherein the  $Nb_3Sn$  superconducting phase was distributed in the form of a continuous network surrounding a second phase.

### Microstructure

A desirable microstructure was obtained by using two variations of the hot press technique. One was a sintering operation performed under a high pressure (8000 psi) at a high temperature (e.g. 1900°C) followed by a lower temperature treatment (1100°C), as shown in Fig. 1(a). The second consisted of hot pressing at a lower temperature (e.g. 500°C) and pressure (e.g. 2000 psi) followed by a high temperature treatment (e.g. 1500°C), as shown in Fig. 1(b). Photomicrographs of the microstructures of two specimens made by the two variations of the hot pressing technique are shown in Fig. 4 and 5. Both specimens had grains of NbC surrounded by a discontinuous network of  $Nb_3Sn$ . Using the first variation, a decrease from about 2000° to 1600°C in the initial temperature appeared to favor the formation of a higher volume fraction of  $Nb_3Sn$ , as shown in Table II. However, specimen number 8, which was made by the second variation, was characterized by a finer grain size. A higher magnification photomicrograph illustrating the finer structure of specimen 8 is shown in Fig. 6. When the initial temperature of reaction was too low, i.e.  $T_1 = 500^\circ C$ , the less desirable

structure shown in Fig. 7 was obtained. A further advantage of using an intermediate value of  $T_1$  (1050°C) was that compounds of niobium and tin, other than that of the desirable  $Nb_3Sn$ , did not form. Small changes in the temperature and time of sintering for either of the two variations had relatively minor effects on the resulting microstructures.

The microstructure of the infiltrated specimens consisted of niobium grains surrounded by a mixture of  $Nb_3Sn$  and  $NbSn_2$ . A typical microstructure is shown in Fig. 8. Microscopic examinations of these specimens showed that the  $Nb_3Sn$  networks were discontinuous.

#### Critical Temperature

The method of preparation of  $Nb_3Sn$  is important because both the superconducting critical temperature and the transition width are influenced by metallurgical variables such as composition and the degree of order.<sup>4 - 10</sup> In the present study, the critical temperature was found to be directly related to the  $Nb_3Sn$  composition. Four sintered specimens (numbered 2, 5, 6, and 9) were examined with the electron beam microprobe and the relation between the chemical composition and the  $T_c$  are given in Table III. As the table shows, the  $T_c$  increases as the composition of the compound approaches the ideal stoichiometry.

It has been shown<sup>8</sup> that  $Nb_3Sn$  exists over a composition range of  $Nb_xSn_{1-x}$ , where  $x = 0.72$  to  $0.80$ , when prepared at 1200°C. Bachner and Gatos<sup>9</sup>, Courtney et al.<sup>10</sup>, and Reed et al.<sup>8</sup> found that above a composition of approximately 80% niobium, the  $T_c$  abruptly decreased to a very low value (about 6°K). Bachner and Gatos<sup>9</sup> surmised that the decrease in  $T_c$  of  $Nb_3Sn$  was due to the volatilization of the tin atoms, with the subsequent migration of niobium atoms to the vacant tin sites in the A-15 crystal structure. This would result in a discontinuity

in the niobium chains, and in the opinion of Reed et al.<sup>8</sup>, the continuity of these chains is the key to the high  $T_c$ . The results of the present study are not inconsistent with the conclusions of these investigators.

The width of transition,  $\Delta T_c$ , is usually an indicator of the degree of nonstoichiometry in the superconducting compound. From the chemical composition and  $T_c$  data given in Table III, no clear correlation between deviation from stoichiometry and  $\Delta T_c$  could be made. However, for the one specimen (number 9) that was very close to ideal stoichiometry,  $\Delta T_c$  was very small. No quantitative correlations between the upper reaction temperatures and the critical temperatures were observed, but specimens prepared at lower reaction temperatures usually had smaller  $\Delta T_c$  values, as can be seen by a comparison of Tables II and IV.

The critical temperatures for specimens prepared by the infiltration technique were typical of stoichiometric  $Nb_3Sn$  and were generally higher than those prepared by the hot press technique. This was probably due to the fact that volatilization of the tin occurred at the high processing temperatures that were used for sintering.

#### Critical Current Density

The critical current density,  $J_c$ , is the most structure sensitive high-field superconducting property. It is not surprising therefore that by the process control used in the present study the critical current density could be varied over a wide range of values. The critical current density,  $J_{cN}$ , is defined as the current density at

which the voltage drop across the specimen reaches the normal state value for a given field. It represents the upper bound for the superconducting state for all fields below the upper critical field,  $H_{c2}$ . The critical current density,  $J_{cS}$ , of a superconductor is the current density at which a voltage drop across the specimen is first detected for a given field. The critical current density,  $J_{cS}$ , could not be determined for any of the specimens above fields of 15 kG because the  $Nb_3Sn$  network was discontinuous and therefore the specimens always had a finite initial resistance. The voltage drop across the specimen observed at low fields was attributed to current conduction in the nonsuperconducting compounds  $NbC$ ,  $Nb_2C$ ,  $Nb_6Sn_5$ ,  $NbSn_2$ , and in tin, which were the phases linking the discontinuous  $Nb_3Sn$ .

The  $J_{cN}$  versus  $H$  curves of some hot pressed specimens are shown in Fig. 9. The current density can be calculated in two ways. One is to use only the cross-sectional area of the  $Nb_3Sn$  phase, and the other is to use the cross-sectional area of the bulk specimen. The current densities obtained in this study are reported in both ways in Table IV. Quantitative metallography was used to determine the approximate area of  $Nb_3Sn$  in the cross-sections of the specimens.

The two specimens prepared by the second variation of the hot press technique (i.e. 8 and 9) had higher bulk current densities for all fields below about 180 kG than specimens 1 through 7. The microstructures of these two specimens were entirely different, as is shown in Fig. 5 and 7. The microstructure of specimen number 8 was characterized by a fine grain size and the presence of only one niobium - tin compound. This specimen had a more uniformly distributed network of

$\text{Nb}_3\text{Sn}$ , which presumably accounted for the higher  $J_{cN}$  values observed for all fields. The influence of elemental tin on the superconducting properties is not known. The low current densities observed at all fields for specimen 2 were evidently due to the nonuniform distribution and unfavorable morphology of the phases, as shown in Fig. 4.

The  $J_{cN}$  versus  $H$  curves are shown in Fig. 10 for an infiltrated specimen and for one of the best hot pressed specimens. The microstructural features of the infiltrated specimens were quite different from those of optimally processed hot pressed specimens, as can be seen by comparison of Fig. 5 and 8. It was a little surprising, therefore, that their properties were so similar.

#### The Upper Critical Field

All the extrapolated values of the upper critical field,  $H_{c2}$ , for both the hot pressed and infiltrated specimens were within the range of about 200 to about 235 kG, as shown in Table IV. These values of  $H_{c2}$  are consistent with those reported by Montgomery and Sampson<sup>11</sup> for bulk material containing  $\text{Nb}_3\text{Sn}$ .

There did not appear to be any correlation between the microstructure and the values of  $H_{c2}$  obtained. This is not surprising because  $H_{c2}$  is known to be largely dependent on  $T_c$  and not on the morphology of  $\text{Nb}_3\text{Sn}$ . The narrow range of  $H_{c2}$  values is consistent with the corresponding narrow spread of  $T_c$  values (less than two degrees Kelvin).

SUMMARY

The microstructure of bulk high-field superconductors was varied by controlling processing variables. Two processes were used - infiltrating a porous niobium compact with liquid tin (liquid phase sintering), and hot pressing of a tin, niobium, carbon powder mixture. The optimum microstructure prepared by both techniques consisted of a network of superconducting phase surrounding other phases. The critical temperature, current carrying capacities, and upper critical fields of a number of specimens were measured. Attempts were made to correlate the measured properties with the observed microstructures.

The critical temperatures for specimens prepared by the infiltration technique were typical of stoichiometric  $Nb_3Sn$  and were higher than most of those prepared by hot pressing. The lower critical temperatures obtained with some hot pressed specimens were probably due to the volatilization of tin at the higher temperatures used.

By appropriate process control the critical current density,  $J_{cN}$ , was varied over a wide range of values. Hot pressed specimen number 8, prepared by an initial low temperature ( $1050^\circ C$ ) sintering treatment followed by a high temperature treatment ( $1900^\circ C$ ), exhibited the highest current carrying capacity. The microstructure of this specimen was characterized by a fine grain size and the presence of only one niobium-tin compound,  $Nb_3Sn$ .

The  $J_{cN}$  versus  $H$  curves of specimens 8 and 10 (hot pressed versus infiltrated) were similar in spite of the fact that their microstructural features were different (because of the differences in chemical composition - one being NbC based, the other Nb based).

All the values of  $H_c$  extrapolated to  $J_{cN} = 0$ , (i.e.  $H_{c2}$ ) for both the hot pressed and infiltrated specimens were within the range of about 200 to about 235 kG. This narrow range of values is consistent with the corresponding narrow spread of  $T_c$  values, i.e. less than two degrees Kelvin.

The results of this study confirm the observations made by previous investigators that the microstructure of bulk high-field superconductors plays an important role in determining values of critical current. The results also suggest that by process control desirable microstructures could be produced which would optimize  $J_{cN}$ .

#### ACKNOWLEDGEMENTS

This work was done under the auspices of the United States Atomic Energy Commission through the Inorganic Materials Research Division of the Lawrence Radiation Laboratory.

TABLE I. Purity, Size and Suppliers of Starting Powders

Material	Purity <sup>(1)</sup>	Powder Size	Supplier
niobium	99.9%	-325 mesh	Kawecki Chemical Company
tin	99.999%	-200 mesh	Cominco Electronic Materials
carbon	< 2 ppm	-	Union Carbide Corporation

(1) Purity as stated by supplier.



TABLE II. Processing Treatments and Estimated  
Percentage of Nb<sub>3</sub>Sn in Microstructure

Specimen Number	Preparation	Temp (°C)	T <sub>1</sub>	Time (min)	Specimen Pressure (psi)	Temp (°C)	T <sub>2</sub>	Time (min)	Specimen Pressure (psi)	%Nb <sub>3</sub> Sn <sup>(1)</sup>
1	Hot Pressed	2030		8	8000	1100		15	8000	3%
2	Hot Pressed	1950		8	8000	1100		60	8000	8%
3	Hot Pressed	1930		8	8000	1100		15	8000	3%
4	Hot Pressed	1840		8	8000	1100		15	8000	-
5	Hot Pressed	1730		8	8000	1100		15	8000	29%
6	Hot Pressed	1730		8	8000	1100		60	8000	12%
7	Hot Pressed	1600		8	8000	1100		60	8000	19%
8	Hot Pressed	1050		30	1000	1880		8	1000	10%
9	Hot Pressed	≈500		15	2000	1500		15	2000	-
10	Infiltrated	≈800		15	1000	1050		2	1000	5%
11	Infiltrated	≈800		15	1000	-		-	-	-

(1) Estimated by lineal analysis.

TABLE III. Critical Temperatures and Electron Probe Microanalysis Results for Selected Hot Pressed Specimens

$T_c$ (°K)	$\Delta T_c$ <sup>(1)</sup> (°K)	Sn in Nb <sub>3</sub> Sn (Atomic %)	Nb in Nb <sub>3</sub> Sn (Atomic %)	Specimen Number
16.4	2.0	21.6	78.4	6
16.7	1.2	22.4	77.6	5
17.3	1.6	24.3	75.7	2
17.8	0.3	24.7	75.3	9

(1)  $\Delta T_c$  is the width of the transition region.

TABLE IV. Superconducting Properties

Specimen Number	$T_c$ (°K)	$\Delta T_c$ (°K)	$H_{c2}^{(1)}$ (kG)	$J_{cN}$ (bulk specimen) at 120 kG(amp/cm <sup>2</sup> )	$J_{cN}$ (Nb <sub>3</sub> Sn only) at 120 kG(amp/cm <sup>2</sup> )	$\rho_n$ (2) (μohm-cm)
1	16.0	2.1	-	-	-	-
2	17.3	1.6	235	1030	12,900	69
3	15.9	1.4	200	1610	53,700	40
4	16.3	3.0	-	-	-	-
5	16.7	1.2	220	1020	3,520	111
6	16.4	2.0	215	800	6,660	120
7	17.8	0.2	-	-	-	-
8	17.2	1.1	230	3000	27,200	24
9	17.8	0.3	215	1700	11,300	48
10	17.6	0.3	225	3400	68,000	4
11	17.6	0.2	-	-	-	-

(1) Extrapolated value to  $J_{cN} = 0$ .

(2)  $\rho_n$  : resistivity of normal sample at 4.2°k

REFERENCES

1. M. L. Picklesimer: U. S. Atomic Energy Commission, 1957, ORNL 2296, Oak Ridge National Laboratory, Oak Ridge, Tenn.
2. E. Nembach: J. Phys. Chem. Solids, 1968, Vol. 29, pp. 1205-1211.
3. M. Suenaga and K. M. Ralls: J. Appl. Phys., 1966, Vol. 37, No. 11, pp. 4197-4200.
4. A. L. Giorgi, E. G. Szklarz, E. K. Storms, A. L. Bowmans, and B. T. Matthias: Phys. Rev., 1962, Vol. 125, pp. 837-838.
5. R. Enstrom, T. Courtney, G. Pearsall, and J. Wulff: Metallurgy of Advanced Electronic Materials, G. E. Brock, ed., pp. 121-150. Interscience Publishers, New York, 1962.
6. H. W. Schadler and H. S. Rosenbaum: J. Metals, 1964, Vol. 16, pp. 97.
7. J. J. Hanak, G. D. Cody, J. C. Cooper, and M. Rayl: Proc. VIII Intern. Conf. Low Temp. Phys., R. O. Davis, ed., pp. 353-354, Butterworths, Washington, D. C., 1963.
8. T. B. Reed, H. C. Gatos, W. J. LaFleur, and J. T. Roddy: Metallurgy of Advanced Electronics Materials, G. E. Brock, ed., pp. 71-87, Interscience Publishers, New York, 1962.
9. F. J. Bachner and H. C. Gatos: Trans. Met. Soc. AIME, 1966, Vol. 236, pp. 1261-1266.
10. T. H. Courtney, G. W. Pearsall, and J. Wulff: Trans. Met. Soc. AIME, 1965, Vol. 233, pp. 212-218.
11. D. Bruce Montgomery and William Sampson: Appl. Phys. Letters, 1965, Vol. 6, No. 6, pp. 108-111.

FIGURE CAPTIONS

- Fig. 1 Schematic of temperatures and times for two variations of the hot pressing process. Specimen pressure equal to 8000 psi.  
(a) Specimen number 2. (b) Specimen number 8.
- Fig. 2 Schematic of temperatures and times for the infiltration process. Specimen pressure equal to 1000 psi.
- Fig. 3 Schematic pulsed field record for specimen number 2. Maximum  $H = 26$  kG and  $J = 3,240$  amp/cm<sup>2</sup>.  $H_{cS}$  is the highest field at which specimen shows zero voltage drop, i.e. is in the superconducting state.  $H_{cN}$  is the field at which the specimen transforms to the normal state. Between  $H_{cS}$  and  $H_{cN}$  the specimen is in the mixed state.
- Fig. 4 Microstructure of specimen number 2 in anodized condition. Phase designation: (1-NbC, 4-Nb<sub>3</sub>Sn, 5-Nb<sub>6</sub>Sn<sub>5</sub>, 7-Sn). Magnification 1000 times.
- Fig. 5 Microstructure of specimen number 8 in anodized condition. Phase designation: (1-NbC, 4-Nb<sub>3</sub>Sn, 7-Sn). Magnification 1000 times.
- Fig. 6 Higher magnification of another area of specimen number 8 (which was shown at a lower magnification in Fig. 5). Phase designation: (1-NbC, 4-Nb<sub>3</sub>Sn, 7-Sn). Magnification 2000 times.

Fig. 7 Microstructure of specimen number 9 in anodized condition.

Phase designation: (1-NbC, 3-Nb, 4-Nb<sub>3</sub>Sn, 5-Nb<sub>6</sub>Sn<sub>5</sub>, 7-Sn).

Magnification 1000 times.

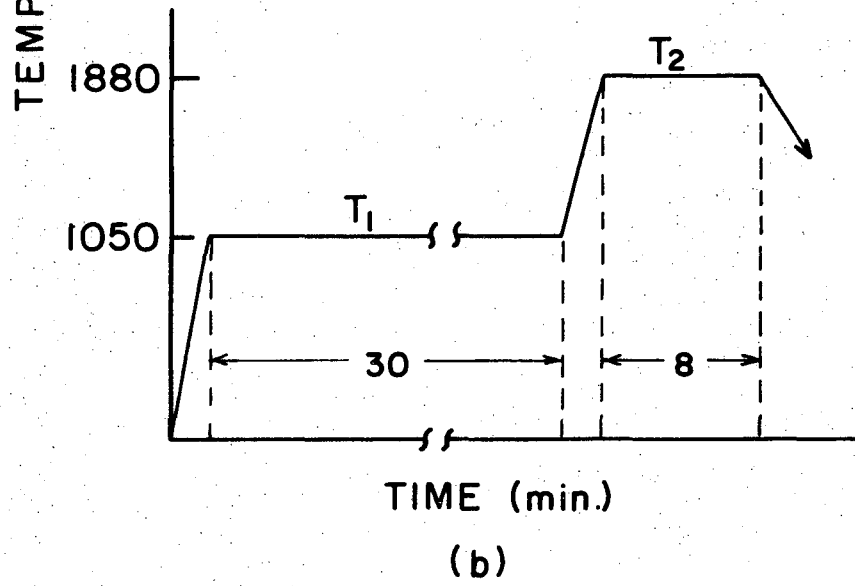
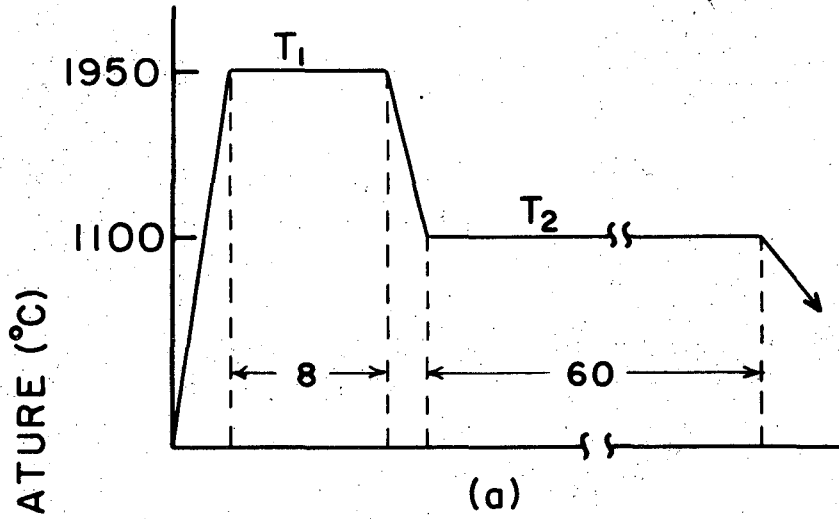
Fig. 8 Microstructure of specimen number 10 in anodized condition.

Phase designation: (3-Nb, 4-Nb<sub>3</sub>Sn, 6-NbSn<sub>2</sub>, 7-Sn). Magnification

1000 times.

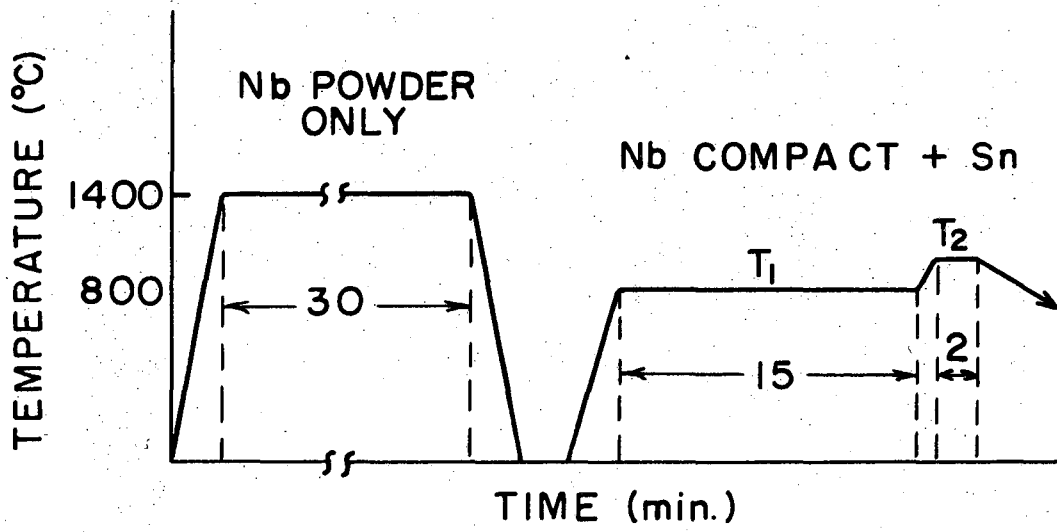
Fig. 9  $J_{cN}$  versus H curves for specimen numbers 2, 8, and 9. The values of  $J_{cN}$  were calculated from the bulk specimen dimensions and the total current.

Fig. 10 Comparison of  $J_{cN}$  versus H curves for a hot pressed specimen (number 8) and an infiltrated specimen (number 10). The values of  $J_{cN}$  were calculated from bulk specimen dimensions and the total current.



XBL 699-5611

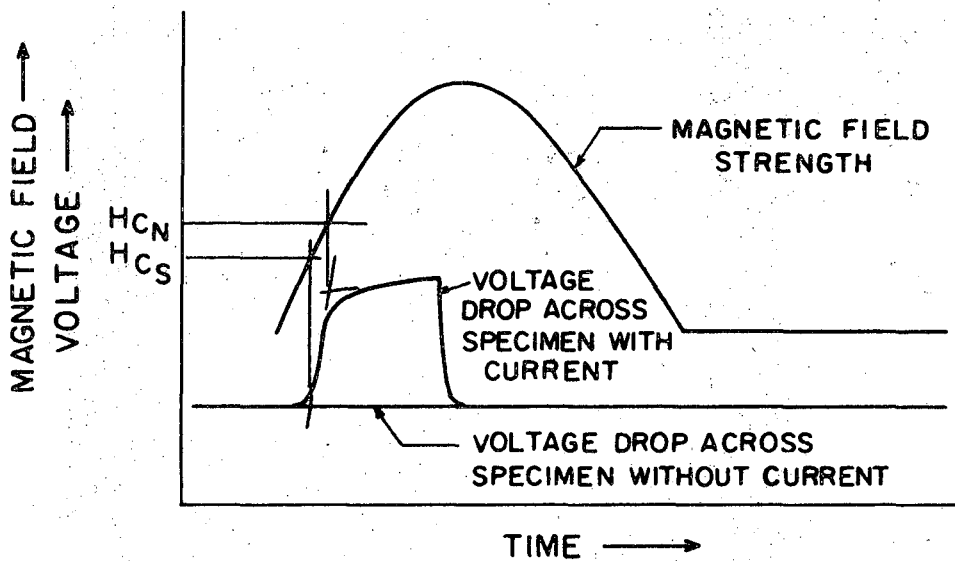
Fig. 1



XBL 699-5667

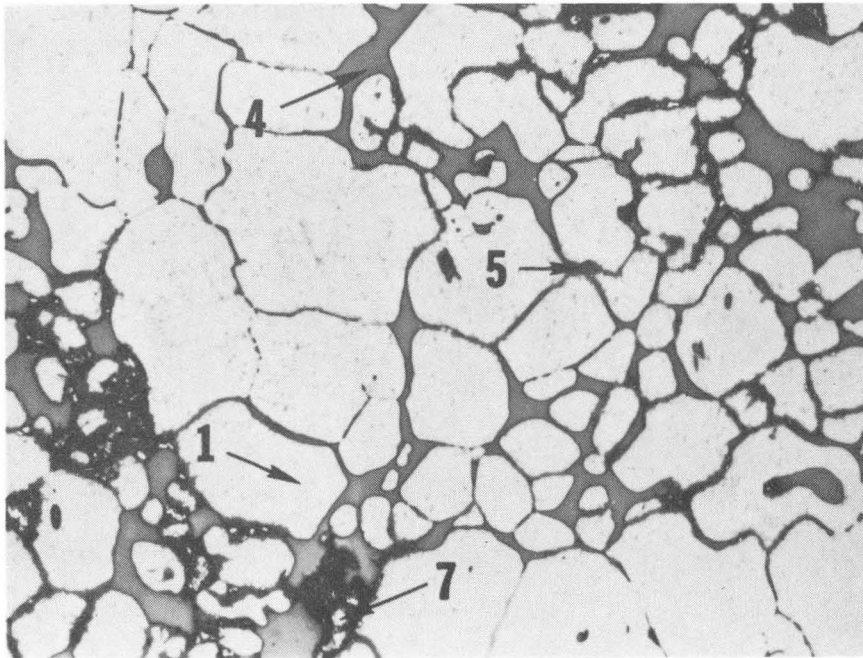
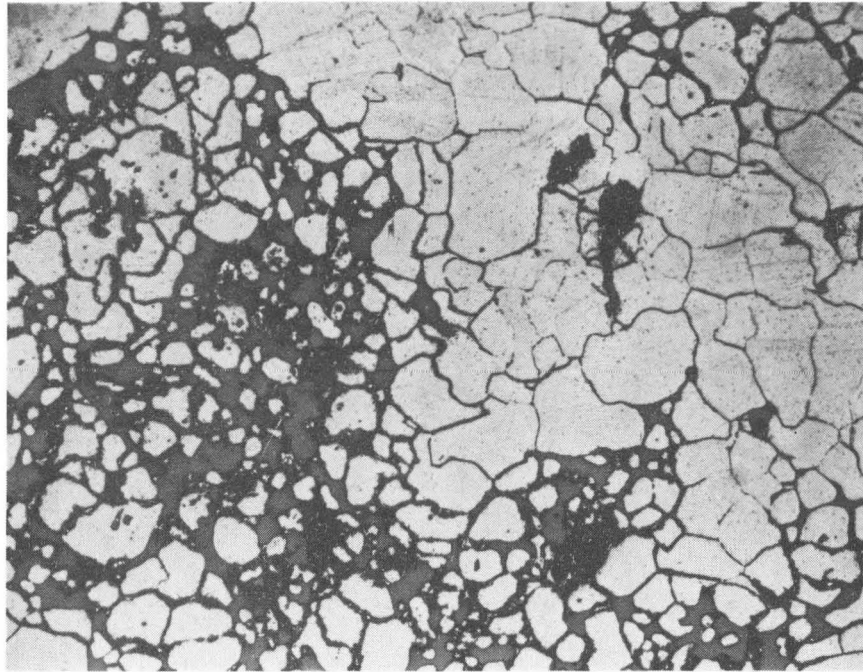
Fig. 2





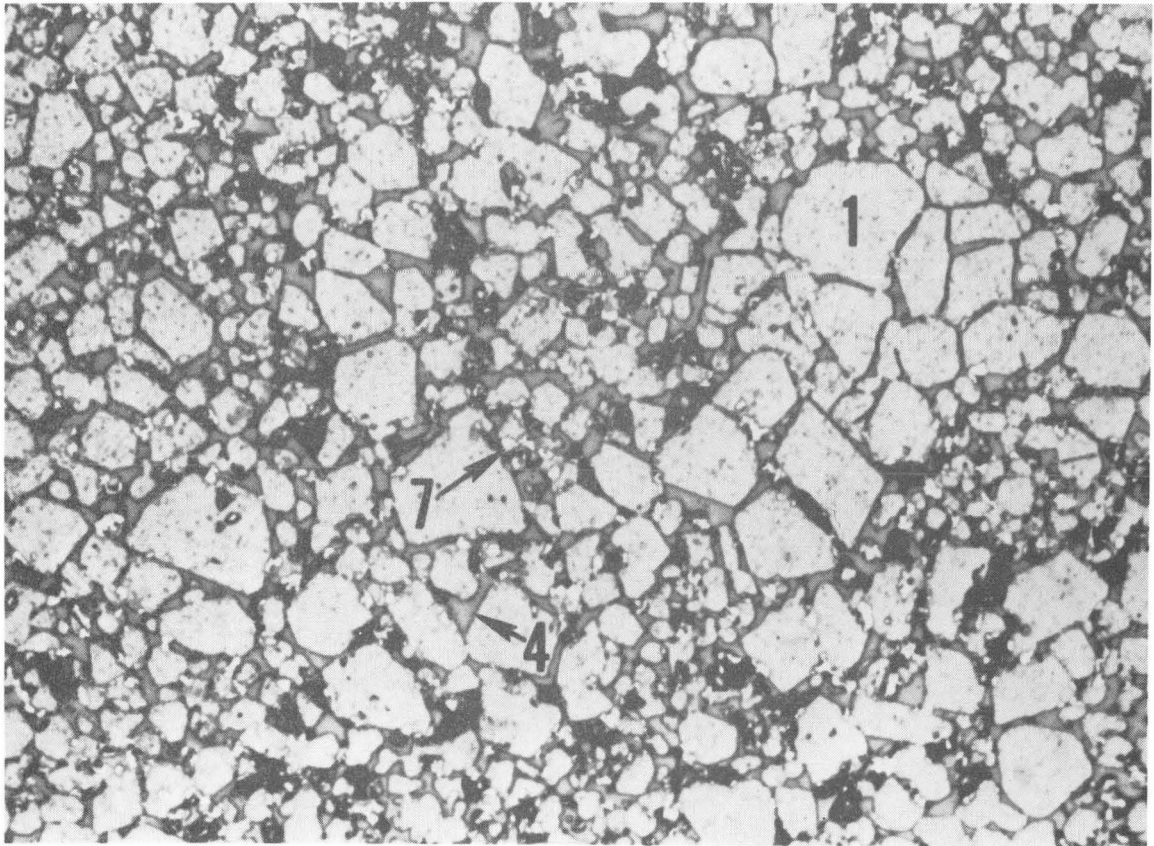
XBL 699-5610

Fig. 3



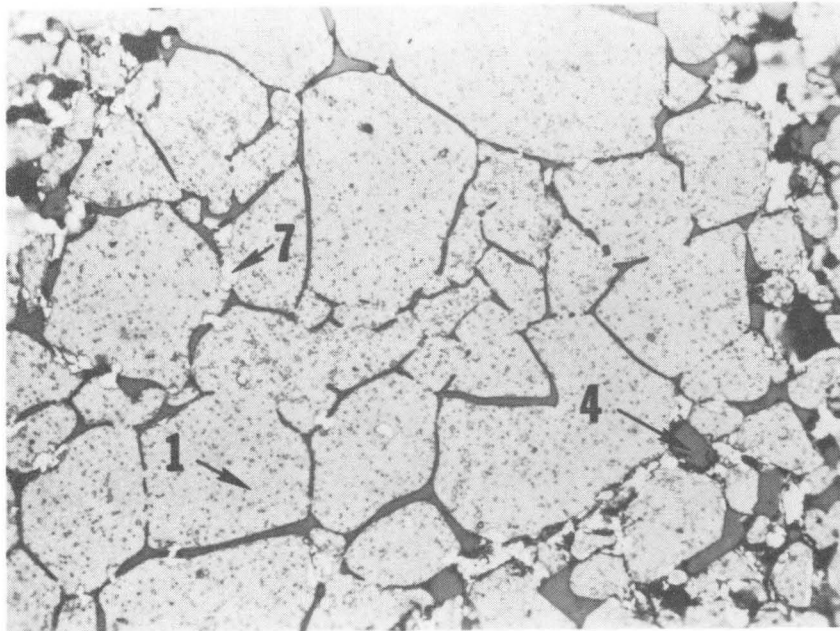
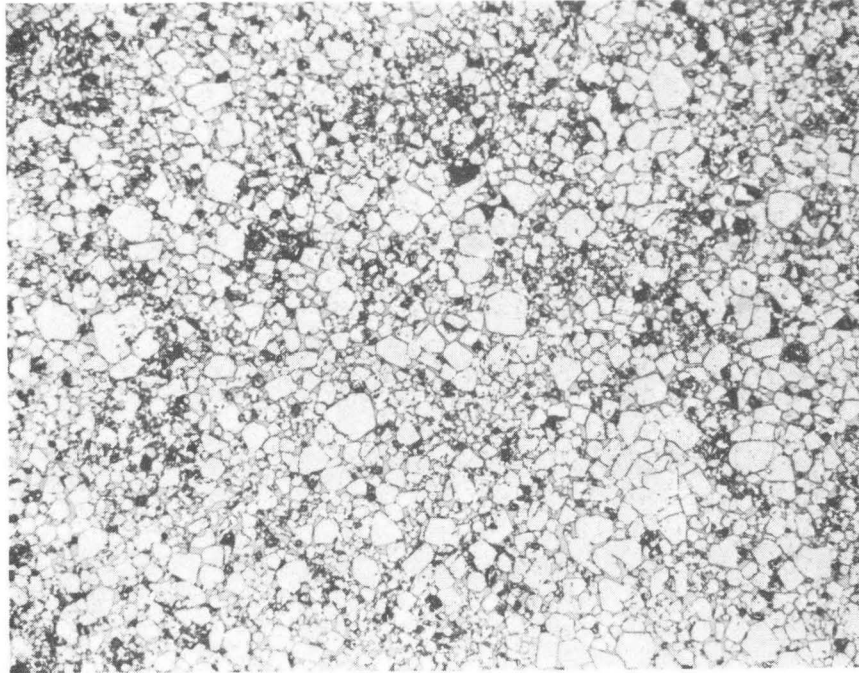
XBB 688-5052

Fig. 4



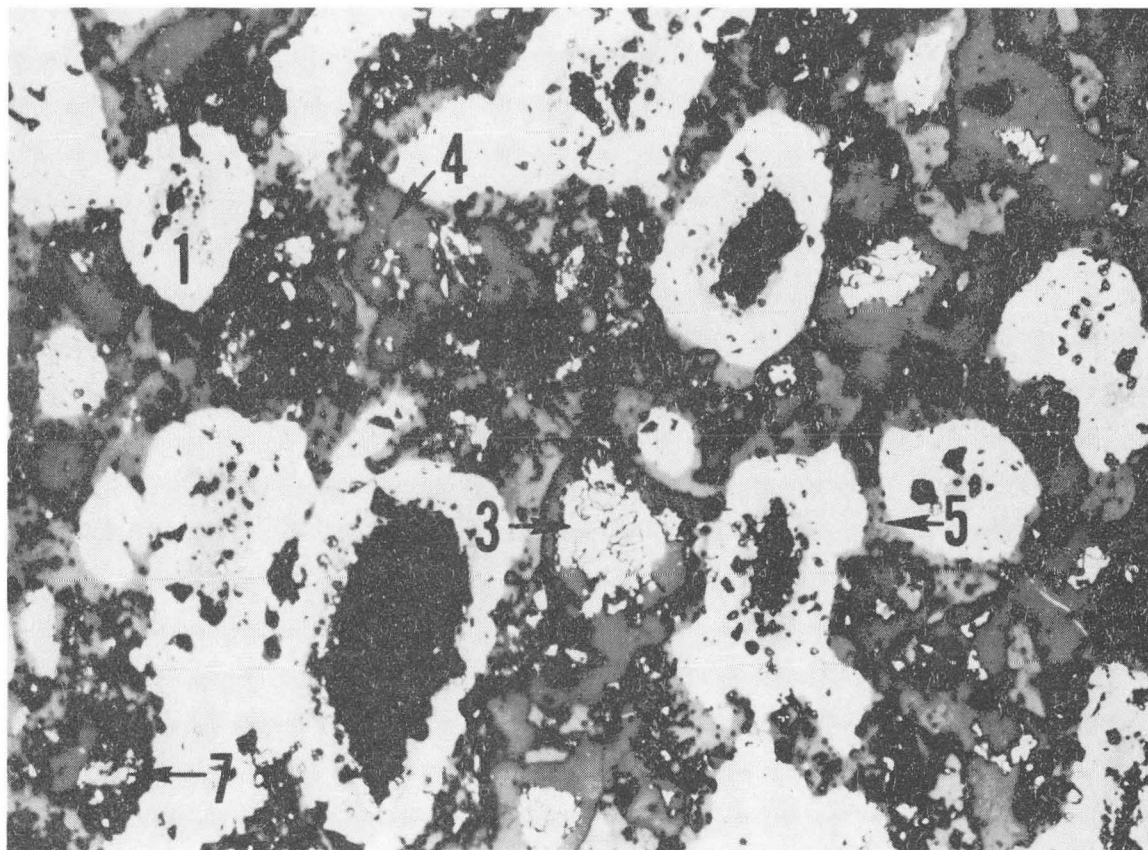
XBB 699-6014

Fig. 5



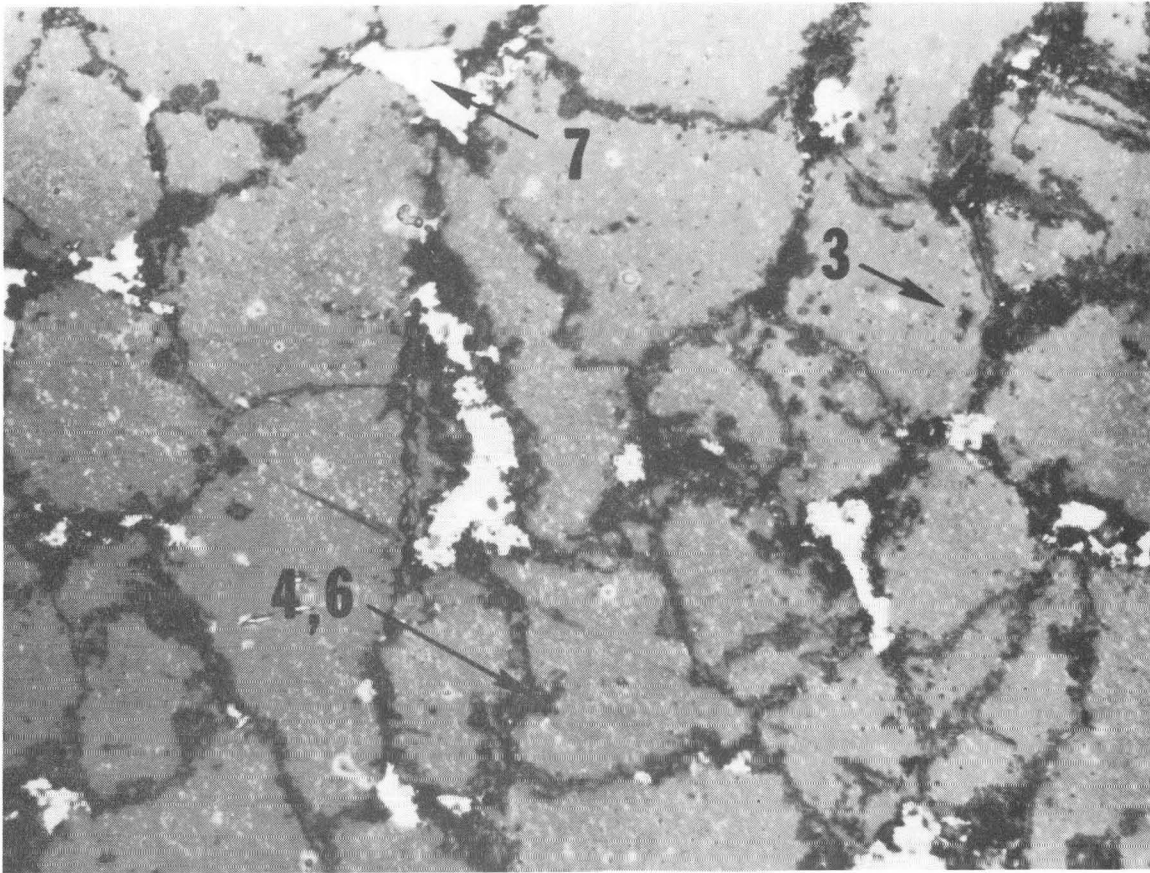
XBB 688-5058

Fig. 6



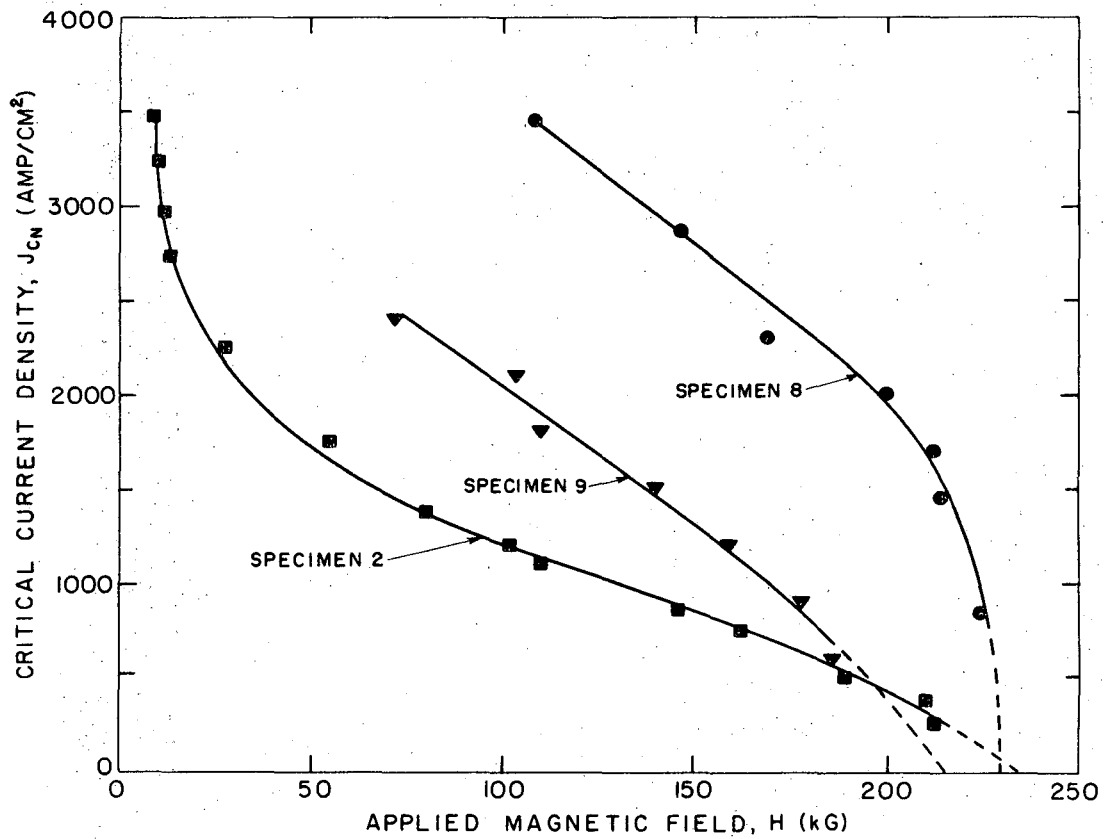
XBB 699-6015

Fig. 7



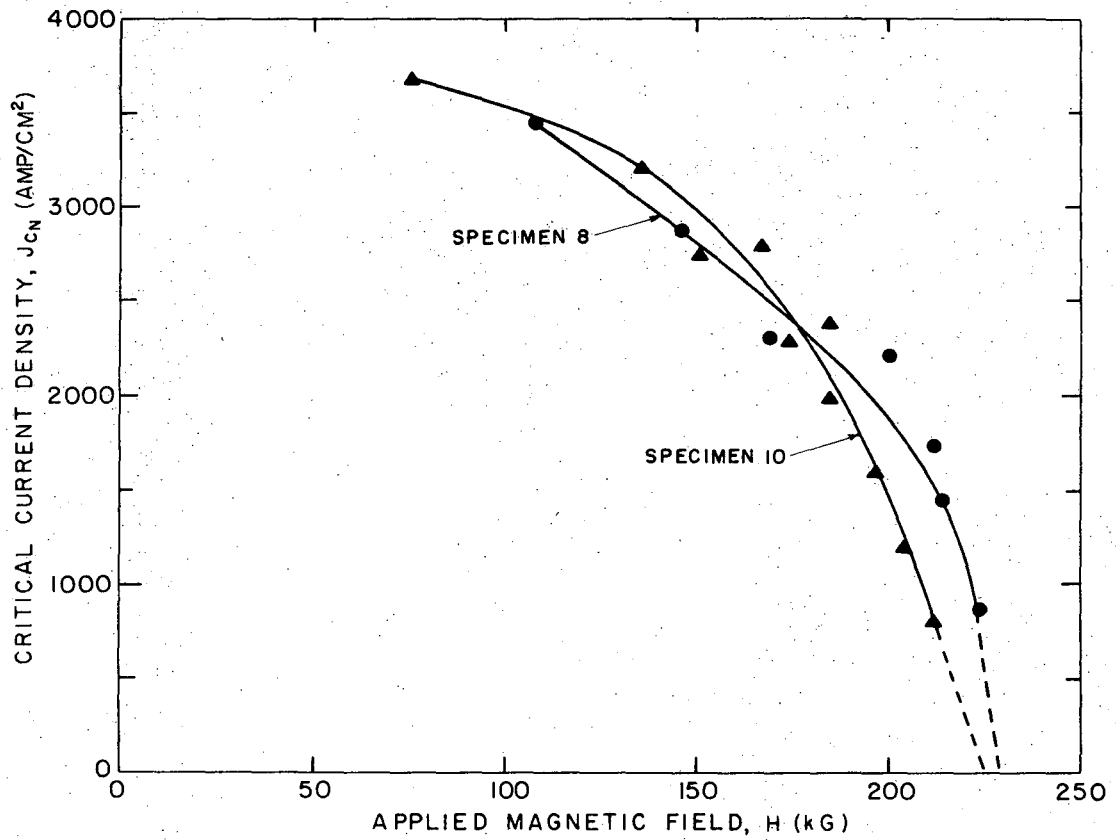
XBB 688-5060

Fig. 8



XBL 699-5612

Fig. 9



XBL 699-5613

Fig. 10



LEGAL NOTICE

*This report was prepared as an account of Government sponsored work. Neither the United States, nor the Commission, nor any person acting on behalf of the Commission:*

- A. Makes any warranty or representation, expressed or implied, with respect to the accuracy, completeness, or usefulness of the information contained in this report, or that the use of any information, apparatus, method, or process disclosed in this report may not infringe privately owned rights; or*
- B. Assumes any liabilities with respect to the use of, or for damages resulting from the use of any information, apparatus, method, or process disclosed in this report.*

*As used in the above, "person acting on behalf of the Commission" includes any employee or contractor of the Commission, or employee of such contractor, to the extent that such employee or contractor of the Commission, or employee of such contractor prepares, disseminates, or provides access to, any information pursuant to his employment or contract with the Commission, or his employment with such contractor.*

TECHNICAL INFORMATION DIVISION  
LAWRENCE RADIATION LABORATORY  
UNIVERSITY OF CALIFORNIA  
BERKELEY, CALIFORNIA 94720